Dynamic Exchange Effects in Broadband Dielectric Spectroscopy

R. Stannarius, F. Kremer, and M. Arndt
Universität Leipzig, Fakultät für Physik und Geowissenschaften, D-04103 Leipzig, Germany
(Received 22 August 1995)

We calculate the consequences of molecular exchange between two states with different relaxation rates in dielectric spectra. In a critical range where exchange rates are of the order of the relaxation rates, both individual processes show apparently increased relaxation frequencies, and the slower process gains intensity from the faster. In the fast exchange limit, only one process with averaged relaxation rate remains. The model is well suited to describe the effects in the dielectric spectra of a microconfined glass-forming liquid (salol) in porous glasses.

PACS numbers: 77.22.Gm

In broadband dielectric spectroscopy, the dynamical behavior of a sample is studied from the analysis of its frequency dependent dielectric function. Data are conventionally interpreted in terms of superimposed Debye, stretched exponential, Havriliak-Negami, or other relaxation functions. The characteristic relaxation frequencies can be related to dynamical processes, e.g., cluster, molecular, or segmental motions. The temperature dependence of a particular relaxation process gives information on mobilities, thermal activation, cooperativity, and glass transition temperatures [1,2].

We consider a sample consisting of two subsystems with different relaxation characteristics, as for example molecules in the bulk and surface layer, respectively, of a sample in confining geometry. Let the dielectric relaxation in each subsystem be characterized by single processes with relaxation rates $s_1 = 1/\tau_1$ and $s_2 = 1/\tau_2$. As long as the molecules of the two subsystems do not exchange during the characteristic time of the measurement (the larger of τ_1 and τ_2), one expects two peaks in the dielectric spectrum, with intensities proportional to the relative occupation numbers in the subsystems. At exchange rates fast compared to τ_1 and τ_2, it is self-evident that only one averaged process will be observed in the dielectric spectrum with a relaxation strength equal to the total of the subsystems.

Here, we study the critical influence of dynamical exchange and the transition from the two-process to a one-process character of the dielectric spectrum if molecules jump randomly between the two subsystems at intermediate rates. For *resonance* processes, these effects are well understood (see, e.g., [3] for NMR spectra). In a simple two line spectrum, transition from slow exchange to fast exchange appears first as a broadening of the two original *resonance* lines and the reduction of their mutual splitting with increasing exchange rate. At intermediate exchange rates, a single line with maximum broadening has formed at the position of the averaged frequency. With still faster exchange, the line broadening reduces again until one sharp line at the averaged frequency remains. In the following we calculate analogous effects on dielectric *relaxation* spectra.

For simplicity, we assume two Debye processes. In absence of exchange, the normalized relaxation functions $\alpha_{1,2}(t) = \exp(-s_{1,2}t)$ describe the behavior of the molecular polarization in states 1 and 2, respectively, in the time domain. The complex dielectric function $\epsilon^*(\omega)$ is related to α via Fourier transform. The relative dielectric strengths are given by the occupation numbers n_1, n_2 of the respective states. First, we consider two equally intensive processes. We analyze the relaxation functions $\tilde{\alpha}_1(t), \tilde{\alpha}_2(t)$ of molecules starting in states 1 and 2, respectively, under the influence of random jumps. The exchange mechanism is a Poisson jump process with jump rate c, where $c_{ij}\delta t$ is the probability that a molecule changes from state i to state j during the infinitesimal time interval δt. For conservation of the occupation numbers $n_1 = n_2$, the jump rates are equal: $c_{12} = c_{21} = c$. The actual shape of the exchange process should be of minor significance for the effects observed in the dielectric data. The important parameter is the rate c which is the inverse of the average time a particle resides in one subsystem without a jump.

The probability of a particle remaining in its original state is $\exp(-ct)$, and a first jump at time t' occurs with a probability density $c\exp(-ct')$. Therefore the relaxation function $\tilde{\alpha}_1(t)$ of all particles starting in state 1 at $t = 0$ is given by the undisturbed relaxation function $\alpha_1(t)$ multiplied by the probability $\exp(-ct)$ that no jump occurred, plus the probability $c\exp(-ct')$ that a particle changes its state at time t' with relaxation $\alpha_1(t')$ before and $\tilde{\alpha}_2(t - t')$ after the jump, integrated over all times $0 \le t' \le t$,

$$\tilde{\alpha}_1(t) = \alpha_1(t)e^{-ct} + \int_0^t \alpha_1(t')ce^{-ct'}\tilde{\alpha}_2(t - t')\,dt'. \tag{1}$$

The function $\tilde{\alpha}_2$ is calculated analogously with permutation of indices 1,2. Inserting $\alpha_i = \exp(-s_i t)$, one ends up with a set of two coupled integral equations,

$$\tilde{\alpha}_1(t) = e^{-(s_1+c)t} + c\int_0^t e^{-(s_1+c)t'}\tilde{\alpha}_2(t - t')\,dt',$$

$$\tilde{\alpha}_2(t) = e^{-(s_2+c)t} + c\int_0^t e^{-(s_2+c)t'}\tilde{\alpha}_1(t - t')\,dt'.$$

 0031-9007/95/75(25)/4698(4)$06.00

Its solution can be readily found after Carson-Heaviside transformation

$$p\int_0^\infty \exp(-pt)f(t)\,dt \equiv \mathcal{L}\{f(t)\} = \phi(p)$$

with the properties

$$\mathcal{L}\{e^{-at}f(t)\} = \frac{p\phi(p+a)}{p+a}$$

$$\text{and } \mathcal{L}\left\{\int_0^t f(t')\,dt'\right\} = \frac{\phi(p)}{p}.$$

The transformed functions $\varphi_i(p) = \mathcal{L}\{\tilde{\alpha}_i(t)\}$ are related to each other by

$$\varphi_1(p) = \frac{p}{p+c+s_1} + \frac{c}{p+c+s_1}\varphi_2(p), \quad (2)$$

$$\varphi_2(p) = \frac{p}{p+c+s_2} + \frac{c}{p+c+s_2}\varphi_1(p). \quad (3)$$

After substitution of (2) in (3), one obtains the solution

$$\varphi_{1,2} = \left[\frac{p(p+r)}{(p+r)^2-q^2}\right] + \frac{c \mp \Delta s}{q}\left[\frac{pq}{(p+r)^2-q^2}\right], \quad (4)$$

where we have introduced

$$s = \frac{s_1+s_2}{2}, \quad \Delta s = \frac{s_1-s_2}{2},$$

$$q^2 = c^2 + \Delta s^2, \quad r = s + c.$$

After inverse transformation into the time domain, the resulting $\tilde{\alpha}_i(t)$ are

$$\tilde{\alpha}_1(t) = e^{-rt}\left(\cosh(qt) + \frac{c-\Delta s}{q}\sinh qt\right), \quad (5)$$

$$\tilde{\alpha}_2(t) = e^{-rt}\left(\cosh(qt) + \frac{c+\Delta s}{q}\sinh qt\right). \quad (6)$$

One can obtain the same results by constructing and solving the matrix rate equations $\dot{\alpha}_i = C_{ij}\alpha_j$. Figure 1 visualizes these functions for $s_2/s_1 = 10$ and three different jump rates c. With exchange, relaxation of the particles initially in the slow state becomes faster and relaxation of those starting in the fast state slows down. At times $\gg 1/c$, one common slope is found for both curves, i.e., the particles "forget" their initial states. The faster the exchange, the sooner both processes couple and reach the averaged slope $s = r - q$. In the experiment, however, one cannot distinguish between contributions $\tilde{\alpha}_1$ and $\tilde{\alpha}_2$. The total relaxation function $\tilde{\alpha}(t) = \tilde{\alpha}_1(t) + \tilde{\alpha}_2(t)$ is shown in the bottom part of Fig. 1. Moreover, in dielectric spectroscopy one usually analyzes $\epsilon(\omega)$ by the fit to empirical relaxation functions. Therefore we rewrite $\tilde{\alpha}(t)$ as a sum of exponential functions and treat the dielectric response as a superposition of Debye processes, where the exponents

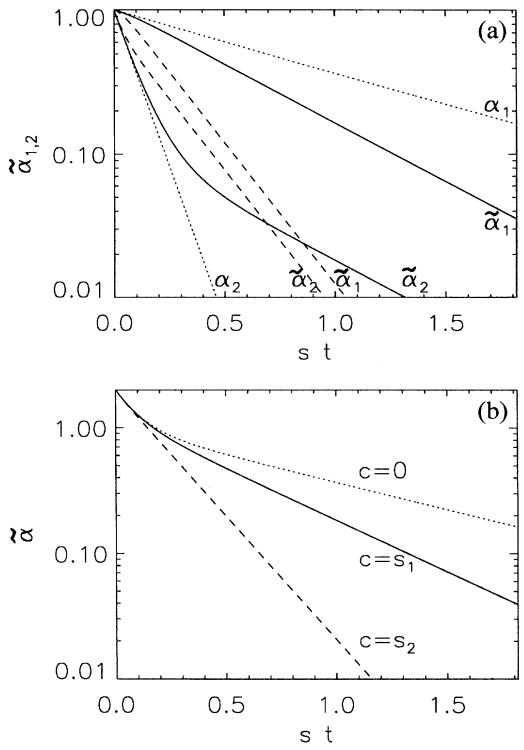

FIG. 1. Top: Relaxation of two Debye processes with $s_2 = 10s_1$ under the influence of a Poisson exchange process with jump rate c according to Eqs. (5) and (6), time axis normalized with the average relaxation rate s. Bottom: sum of both relaxation curves $\tilde{\alpha} = \tilde{\alpha}_1 + \tilde{\alpha}_2$ [Eq. (8)]. Dotted lines: no exchange, $c = 0$; solid lines: $c = s_1$; dashed lines: $c = s_2$.

give apparent relaxation frequencies and the factors represent the apparent dielectric strengths,

$$\tilde{\alpha}(t) = \left(1 + \frac{c}{q}\right)e^{-(r-q)t} + \left(1 - \frac{c}{q}\right)e^{-(r+q)t}. \quad (7)$$

One realizes that the relaxation function in the presence of dynamical exchange can be interpreted as a sum of two exponentials. In the limit $c = 0$ (no exchange), the exponents are equivalent to the original rates s_1 and s_2. With increasing c, both relaxation rates shift to higher values (faster relaxation). The fast rate diverges with $s + 2c$ in the limit $c \to \infty$, whereas the slow rate asymptotically approaches the average s. With increasing exchange, the fast process rapidly loses its apparent intensity $(1 - c/q)$, the slow process gains intensity $(1 + c/q)$ and comprises the total intensity at $c \to \infty$.

Figure 2 depicts the scenario for $s_2 = 100s_1$, where the horizontal axis denotes the logarithmic relaxation time, and the height of the vertical bars correspond to apparent dielectric strength. Note the difference in the behavior of resonance lines described above. When the dielectric spectra are analyzed in terms of Debye [or Kohlrausch-Williams-Walts (KWW), Havriliak-Negami, etc.] functions [4–8], one observes two apparent processes with

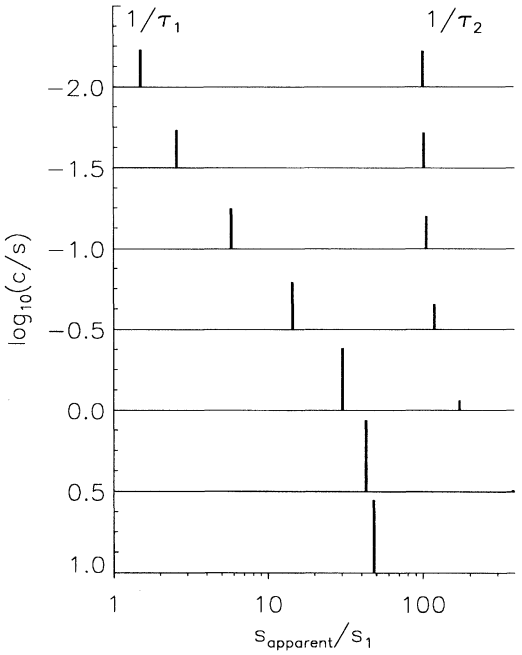

FIG. 2. Two dielectric relaxation processes with $s_2 = 100s_1$ under the influence of mutual exchange with jump rate c. The height of the vertical bars denotes their apparent relaxation strengths, and the horizontal positions give their relaxation rates as given in Eq. (7).

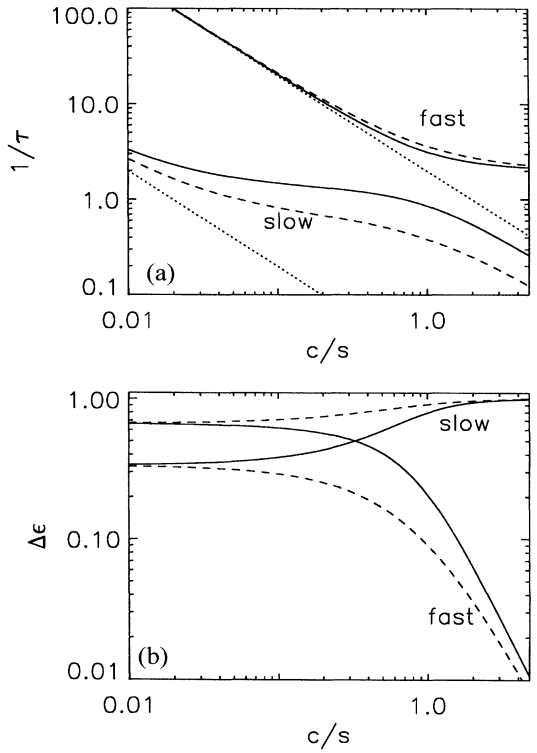

FIG. 3. Top: apparent relaxation rates $1/\tau$ (in arbitrary units) of two processes with relaxation time ratio $s_2/s_1 = 100$ at fixed exchange rate c, and s slowing down from left to right. The dotted lines visualize the assumed exponential decrease of the undisturbed rates s_1 and s_2. The relative strengths of the original fast and slow processes are 1 : 2 (dashed line) and 2 : 1 (solid line) respectively. $(\Delta c/c = (n_1 - n_2)/(n_1 + n_2) = \pm 1/2)$. Bottom: The apparent relaxation strengths $\Delta\epsilon$, notation as above. The relative strength of the slow process approaches 1, the fast process strength decays to zero with increasing exchange, irrespective of the strengths of the uncoupled processes.

both relaxation rates increasing with faster exchange, connected with a transfer of dielectric strength from the fast to the slow process. It has to be noted at this point that similar effects are well known from the behavior of NMR longitudinal and transverse relaxation times [9,10], and the corresponding equations can be directly adopted.

Without derivation we add here the solutions for two subsystems with different intensities due to different occupation numbers n_1 and n_2 states 1 and 2. The jump rates c_{12} and c_{21} are now different and fulfill the conservation condition $c_{12}n_1 = c_{21}n_2$. We introduce

$$\Delta c = \frac{c_{12} - c_{21}}{2}, \quad c = \frac{c_{12} + c_{21}}{2},$$
$$Q^2 = c^2 + \Delta s^2 + 2\Delta s \Delta c\,.$$

Similarly to Eq. (7), we obtain

$$\tilde{\alpha}(t) = \left(\frac{1}{2} + \frac{c}{2Q} + \frac{\Delta c \Delta s}{2Qc}\right)e^{-(r-Q)t} + \left(\frac{1}{2} - \frac{c}{2Q} - \frac{\Delta c \Delta s}{2Qc}\right)e^{-(r+Q)t} \qquad (8)$$

for the complete relaxation function (sum of relaxation strengths normalized to 1).

Typical graphs are visualized in Fig. 3, where a different representation than in Fig. 2 is chosen to allow for straightforward comparison with the experimental data below. We keep the exchange rate constant and lower the relaxation rates $s_1, s_2 = 100s_1$ exponentially from left to right (dotted lines) to model typical slowing down of relaxation rates with decreasing temperature. In the top part, the curves represent the apparent relaxation rates $r \pm Q$; in the bottom part of the figure, the apparent relaxation strengths $\frac{1}{2} \mp (\frac{c}{2Q} + \frac{\Delta c \Delta s}{2Qc})$ are shown in logarithmic scale. The apparent shift to higher relaxation frequencies is of course only an effect of conventional data interpretation. Molecules starting in the fast relaxation state do not relax faster by exchange with a dynamically slower state. This is easily verified from the graphs in Fig. 1 or by calculating the time derivatives of $\tilde{\alpha}_i(t)$.

These theoretical results can be used to interpret recent experimental dielectric data of salol (*phenylsalicylate*) confined in porous sol-gel glasses [11]. In bulk salol, one observes a single relaxation process. Its relaxation rate decreases with lower temperatures (with VFT behavior). Dielectric bulk data are given by stars in Fig. 4. When

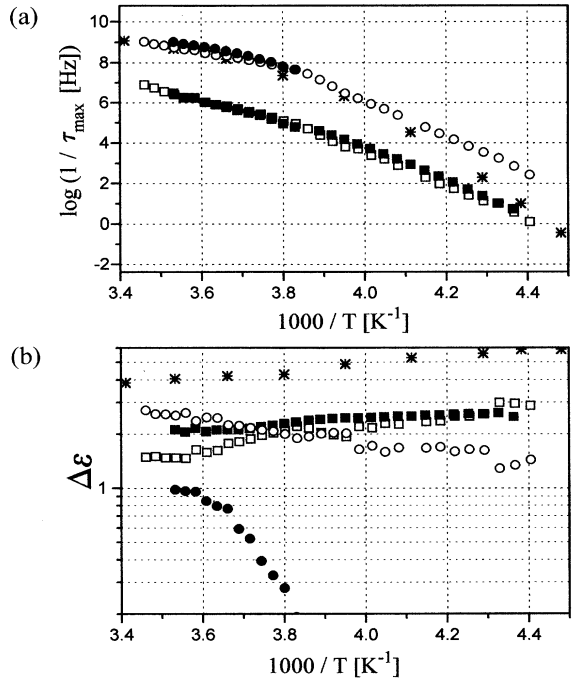

FIG. 4. Dielectric strength $\Delta\epsilon$ and relaxation rate $1/\tau$ of salol in the bulk (stars) and in porous sol-gel glass of 7.5 nm (open symbols) and 2.5 nm (filled symbols) diameter. Circles and squares denote the volume and surface processes, respectively. Note the excellent qualitative agreement of the curves marked by open symbols here with the solid lines in Fig. 3, as well as those marked by filled symbols with the dashed lines in Fig. 3.

salol is adsorbed to porous glass with nanometer pore diameters, new characteristic features are observed. One process, which can obviously be attributed to the free salol in the pores, at high temperatures shows a relaxation rate equal to that of the bulk, but with decreasing temperature it becomes faster than bulk relaxation at comparable temperatures. A second process, attributed to a layer of surface bound salol, appears at relaxation rates almost two decades slower. With lowering temperature, it gradually approaches the bulk rate. (A third process at very low frequencies, due to Maxwell-Wagner polarization, will not be considered here and has been omitted in the representation.) As temperature reaches the vicinity of the glass transition, the fast (volume) process loses its dielectric strength. The second (surface) process gains strength such that the sum of both processes roughly follows the temperature curve of the bulk value. Comparison with Fig. 3 suggests the following interpretation: Both the surface and volume relaxation rates in the pores are fast compared to the molecular exchange process between surface bound and free salol at high temperatures. Their ratio is roughly 1 : 100. On the basis of the ratio of pore radii and molecular sizes $\approx$0.5 nm, one expects that the ratio of free salol in the pores to the amount of salol molecules bound in a monomolecular surface layer is 1 : 2 and 3 : 1 for pore diameters of 2.5 nm and 7.5 nm, respectively. This is roughly equal to the respective experimental high temperature ratios of the dielectric strengths. As the temperature is lowered towards the glass transition, dielectric relaxation rates reach the order of magnitude of the exchange rate between free and surface bound salol, which has a weaker temperature dependence. We make use of the reasonable assumption that the relaxation rate of free salol in the pores obeys the temperature behavior of the bulk liquid. Now, the predictions of the exchange model derived above take effect. With decreasing temperature, random exchange between surface layer and free molecules leads to an apparently faster relaxation of the fast (volume) process compared to the bulk curve, and also to an increased rate of the slow (surface) process, which gradually comes near to the bulk curve. The measured relaxation strengths also show exactly the predicted behavior; the slow process apparently gains intensity from the fast process. These preliminary discussions are certainly only qualitative, because we have no quantitative information on the exchange rates. Nevertheless, the theory describes with great precision all effects observed experimentally.

Summarizing, we have presented a theoretical description of exchange effects on two-process dielectric relaxation spectra. We have shown that experimental data obtained for salol in microporous glasses can be interpreted in terms of a surface-volume exchange of salol molecules on the characteristic time scale of the dielectric experiment. This promising approach has stimulated further dielectric and NMR experiments on microconfined glass-forming liquids, which are now being performed to allow for a quantitative determination of the molecular parameters involved and the proof of this interpretation of the dielectric spectra obtained from microconfined glass-forming liquids.

We gratefully acknowledge support from the Sonderforschungsbereich SFB294.

[1] A. Schönhals, F. Kremer, and E. Schlosser, Phys. Rev. Lett. **67**, 999 (1991).
[2] A. K. Jonscher, *Dielectric Relaxation in Solids* (Chelsea Dielectrics Press, London, 1983), p. 100ff.
[3] A. Abragam, *The Principles of Nuclear Magnetism* (Clarendon Press, Oxford, 1961), Chap. X.
[4] S. Havriliak and S. Negami, J. Polym. Sci. C **14**, 99 (1966).
[5] S. Havriliak and S. Negami, Polymer **8**, 161 (1967).
[6] R. Kohlrausch, Ann. Phys. (Leipzig) **12**, 393 (1847).
[7] G. Williams and D. C. Watts, Trans. Faraday Soc. **66**, 80 (1970).
[8] F. Alvarez, A. Alegria, and J. Colmenero, Phys. Rev. B **44**, 7306 (1991).
[9] D. E. Woessner, J. Chem. Phys. **35**, 41 (1961).
[10] H. Pfeifer, Nucl. Magn. Res.-Basic Principles and Progress **7**, 55 (1972).
[11] M. Arndt and F. Kremer, Mater. Res. Soc. Symp. Proc. **366**, 259 (1995).